Intermittency and coherent structures in the two-dimensional inverse energy cascade: Comparing numerical and laboratory experiments

T. Dubos and A. Babiano
Laboratoire de Météorologie Dynamique, École Normale Supérieure, 24 rue Lhomond, 75005 Paris, France

J. Paret and P. Tabeling
Laboratoire de Physique Statistique, École Normale Supérieure, 24 rue Lhomond, 75005 Paris, France

(Received 17 November 2000; revised manuscript received 2 May 2001; published 29 August 2001)

We study the internal intermittency in the inverse energy cascade and in the condensation regime of two-dimensional turbulence, using physical and numerical experimental approaches. The analysis confirms that the velocity increments have nearly Gaussian distributions at all scales in the inverse cascade regime; it moreover shows that, in the condensation regime, the probability distribution functions of the velocity increments are non-Gaussian but do not significantly vary with the scale; it follows that one may consider that there is essentially no intermittency (in the usual sense), in the condensation regime. In both regimes, we emphasize that coherent structures (i.e., long-lived vortices) are clearly visible on the vorticity field, and we suggest the non-Gaussianity of the distributions in the condensation regime is due to the presence of a large-scale long-lived structures. The study is supplemented by the analysis of the distribution of energy transfers at various scales.

DOI: 10.1103/PhysRevE.64.036302 PACS number(s): 47.27.Eq, 05.45.−a

I. INTRODUCTION

Recent experiments, performed in soap films [1], in mercury [2], and in shallow layers of electrolyte [3], have confirmed theoretical proposals, made long ago by Kraichnan [4], on the inverse energy cascade in two-dimensional turbulence. In particular, an inertial range in which Kolmogorov-Kraichnan $k^{-5/3}$ spectral law holds was convincingly obtained in these studies. There seems to be little doubt now that the inverse energy cascade dynamics can be developed in physical systems when three-dimensional perturbations are maintained at sufficiently low level and, consequently, when three-dimensional effects enter as a negligible factor compared with the constraint imposed by basic quadratic invariants of two-dimensional (2D) motion. These experimental results agreed well with earlier direct numerical simulations [5–8], which consistently conveyed numerical evidence concerning Kraichnan's prediction. Moreover, laboratory and numerical investigations concluded that intermittency in the two-dimensional energy cascade regime is very weak [7–9]. This fact has been observed in forced 2D numerical experiments dissipated at large scale [7]; it was also observed in the early nonstationary simulations of Ref. [10,11]. This is a quite surprising property of the 2D turbulent dynamics, compared the 3D direct energy cascade, which diplays internal intermittency.

It seemed to us worthwhile to investigate whether there is internal intermittency in the condensation regime, i.e., when friction is so low that energy piles up at a wave number comparable to the box wave number, a situation anticipated by Kraichnan long ago [4]. Condensation regimes are characterized by the presence of large-scale long-lived structures, which, in the litterature, are often suspected as sources of intermittency (albeit in a loose sense). It is thus interesting to investigate that sort of contribution they can make in this respect, and whether they may favor the buildup of internal intermittency, in a system where the energy transfers are presumably nonintermittent.

The purpose of the present study is to thus address this question from both numerical and physical points of view. For completeness, we also study in the numerical case the pair distribution function (PDF) of energy fluxes. The latter approach is not feasible yet in laboratory experiments due to the difficulty of obtaining a proper determination of the pressure field.

II. EXPERIMENTS AND ANALYZING TOOLS

A. Numerical experiments

The numerical procedure is described in more detail in [7]. In the numerical approach, we simulate the two-dimensional motion of an incompressible fluid by solving the vorticity equation on a doubly periodic square domain of size $2\pi\times 2\pi$ using a pseudospectral approximation [12]:

$$\partial_t \omega + J(\omega,\psi) = F_\omega - D_\omega, \tag{1}$$

where $\omega = \mathrm{curl}\,\vec{v}$ is the vorticity component orthogonal to plane of motion, ψ the stream function, J the two-dimensional Jacobian operator, F_ω an external vorticity source, and D_ω the vorticity sink associated with dissipation. The latter is the sum of a large-scale linear friction and a small-scale dissipation. Forcing is achieved by keeping constant the amplitude of a given Fourier mode k_I.

In the sequel, we will consider three different numerical experiments with various resolutions and configurations:

(1) (DNS.I) 1024×1024 grid simulation forced at a large wave number $k_I = 256$ and dissipated by the *anticipated potential vorticity method* at small scale [12] and by linear friction at large scale; this simulation presents a well developed inverse energy cascade in statistically steady state where the $k^{-5/3}$ behavior is observed through one decade [7].

(2) (DNS.II) 512×512 grid simulation forced at a smaller wave number $k_I=40$ and dissipated by the iterated Laplacian method (Δ^8) at small scale and by linear friction at large scale; this simulation presents a stationary energy cascading range roughly consistent with a $k^{-5/3}$ behavior in which coherent vortices are more intense and higher in size compared to the experiment (DNS.I).

(3) (DNS.III) 256×256 grid simulation forced at $k_I=30$ and dissipated by the Δ^8 iterated Laplacian method at small scale while the large scale friction is set to zero. This simulation presents a nonstationary evolution of the inverse energy cascade characterized by a growth of the vortical structures and an accumulation of the turbulent kinetic energy at the largest scales of motion with a k^{-3}-compatible energy spectrum. This simulation shows coherent vortices having characteristic sizes encompassing the energy-cascading range: one can see in Fig. 1 vortices with sizes ranging from the injection scale to a fraction of the box size for the largest two of them.

B. Laboratory experiments

The laboratory experiment is described in some detail in [3]. The flow is generated in a PVC cell filled by two layers of NaCl solution, the heavier underlying the lighter. This stable stratification enables a two-dimensional behavior. The dissipation is provided by fluid viscosity and friction exerted by the bottom wall on the fluid. The conductive fluid is forced by an electric current (driven through the cell from one side to another) coupled to a magnetic field (produced by permanent magnets located just below the bottom of the cell). We shall consider two different experiments:

(1) (LE.I) This experiment, studied in detail in [9], exhibits a stationary regime, and spectral properties similar to the simulation (DNS.I). It displays a $k^{-5/3}$ behavior over a range slightly narrower than one decade.

(2) (LE.II) In this experiment, accumulation of energy at large scales is achieved by increasing the depth of the liquid layer, thus decreasing the bottom friction. In this case, the flow structure is organized by a single intense vortex. The velocity spectrum is characterized by a peak at the lowest available wave number and is consistent with a k^{-3} spectral law [13]. This flow is to be compared with the numerical flow (DNS.III).

Figure 1 shows vorticity levels for the numerical experiments. Typical stream functions of the laboratory experiments are displayed in [3] (Figs. 5 and 17). We also display in Fig. 2 vorticity cross sections for experiments (LE.I) and DNS I, II, and III. A vorticity cross section for experiment (LE.II) can be found in [3] (Fig. 19). It can be clearly observed that in experiments (LE.I), (LE.II), and (DNS.I) the highest vorticity values are about two to eight times the root-mean-square deviation ω_{rms} of ω. Conversely the intense vortices of experiments (DNS.II) and (DNS.III) are characterized by a vorticity value at the core larger than 15 or even 20 times ω_{rms}.

C. Analyzing tools

From the measurement of the velocity field, one can calculate the *probability distribution function* $P_l(\delta v_\parallel)$ of the two-point velocity differences longitudinal to the separation vector $\vec{l}$ and the *hyperflatness factors* of the longitudinal velocity increments as a function of $l=||\vec{l}||$. They are defined by the following relations:

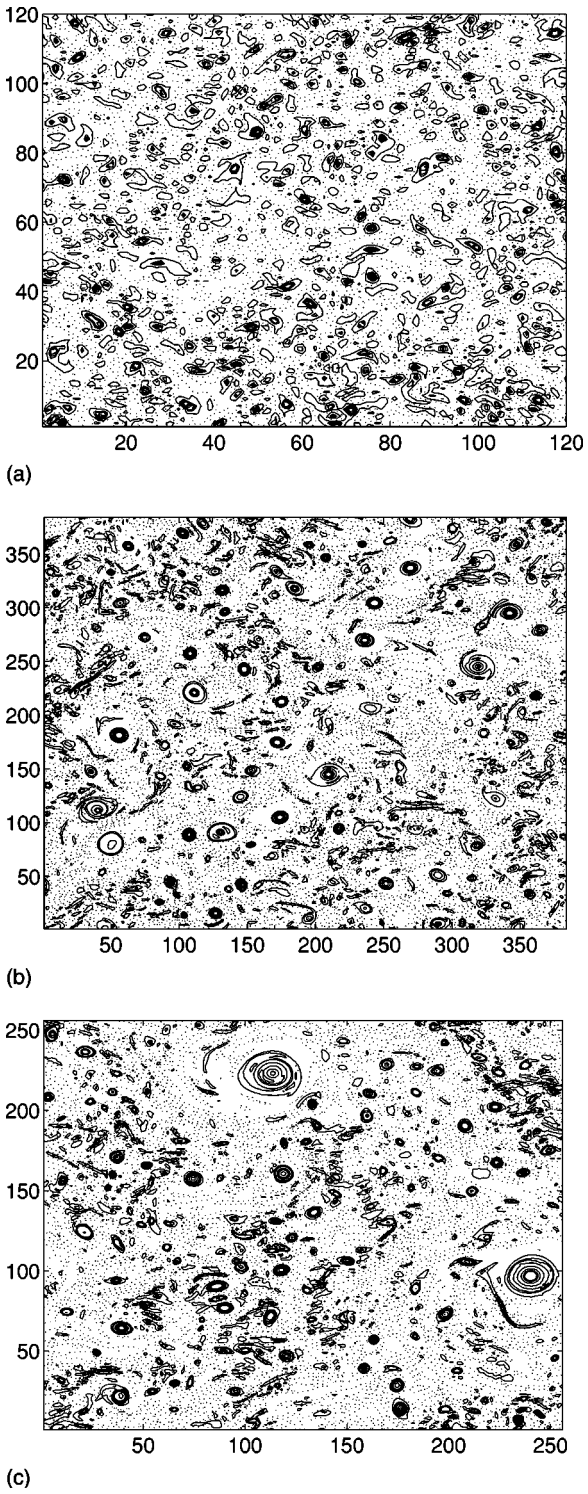

FIG. 1. Isovorticity levels for numerical experiments (a) DNS I, (b) II, (c) III: $\omega=0$ (dotted), $|\omega|\geq\omega_{rms}$ (solid). The boxes shown are 60-injection scales wide.

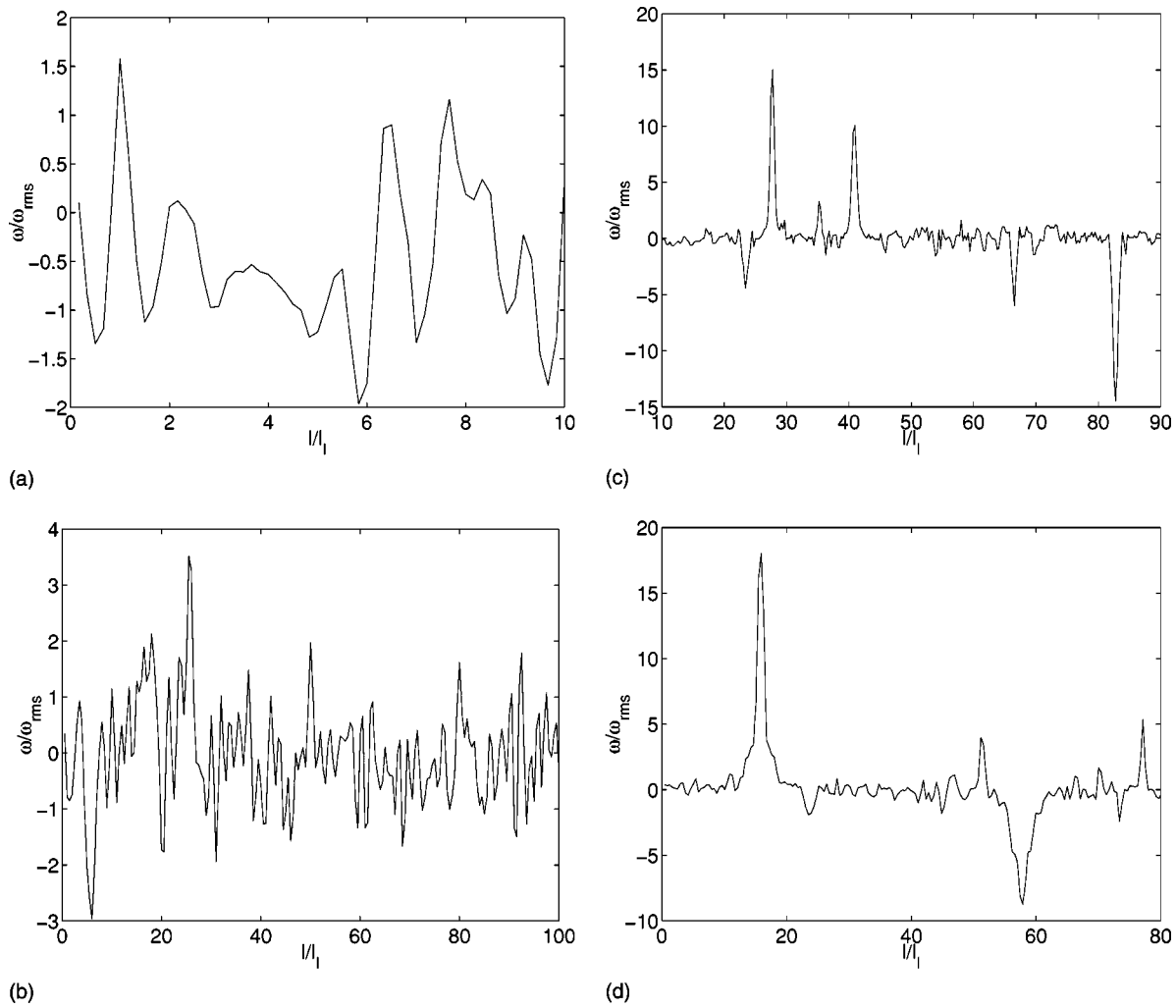

FIG. 2. Typical vorticity profiles across vortices in experiments; (a) (LE.I); (b) DNS I; (c) II; and (d) III.

$$H_{2n}(l)=\frac{S_{2n}(l)}{S_2(l)^n}, \tag{2}$$

where the structure function is defined as

$$S_n(l)=\langle \delta v_{\parallel}(l)^n\rangle=\int_{-\infty}^{+\infty} P_l(v)v^n \mathrm{d}v, \tag{3}$$

$\delta v_{\parallel}$ is the longitudinal velocity increment at the separation distance l. In the above relation, the brackets mean average over the entire flow field, over the direction of $\vec{l}$ and in time. For the unsteady experiment (DNS.III) we averaged over a time period of 200 turnover times, which is small compared to the time scale for the evolution of the energy spectrum. For the experiment (LE.II) the averaging in time is performed while the total circulation remains constant. As in [9], we restricted ourselves to moment orders n such that the function $P_l(v)v^n$ is smooth within the resolved range of $\delta v_{\parallel}$.

These statistical quantities measure different phenomena. The correct criterion for intermittency stems from the shape dependence of the PDF with l, a constant shape indicating the absence of intermittency. Indeed, a constant shape is equivalent to l-independent values of H_{2n}. With $S_{2n}(l)=H_{2n}S_2(l)^n$ and $S_n(l)\propto l^{\zeta_n}$ one gets $\zeta_{2n}=n\zeta_2$ and no intermittency correction to the linear law $\zeta_n\propto n$.

On the other hand, hyperflatness factors only measure the deviations of the PDF from the Gaussianity (breadth of PDF tails) since they can be compared to the Gaussian expectation $H_{2n}=(2n)!/2^n n!$. Velocity statistics may be in principle non-Gaussian and still nonintermittent (l-independent shape of the PDF, and therefore constant values of H_{2n}, $H_{2n}=\text{const}\neq(2n)!/2^n n!$).

From a viewpoint more connected to the cascade concept, the intermittency can also be questioned by a direct study of the energy flux defined in physical space [14]. The flux φ_l is defined by

$$\varphi_l=\oint_{\Sigma_l}\left(\frac{v^2}{2}+p\right)\vec{v}\cdot\vec{n}\,\mathrm{d}s, \tag{4}$$

where p is the pressure and $\vec{n}$ is the outwards oriented unit vector normal to the control contour Σ_l with typical size l. Since $\vec{n}$ is outwards oriented, a positive value of φ_l is con-

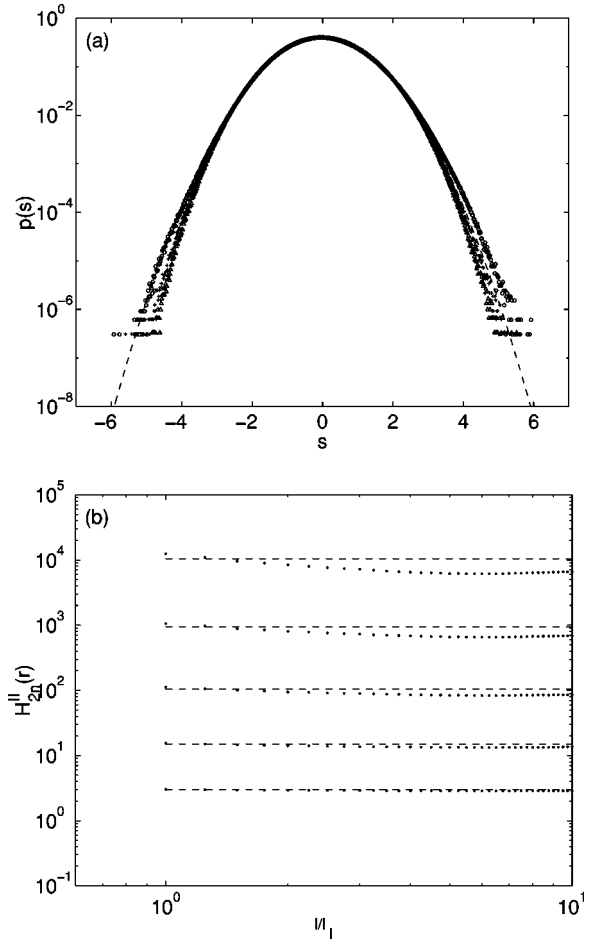

FIG. 3. (a) Rescaled PDFs of longitudinal velocity increments for three different separations ($\ell/\ell_I=2,5,10$) in the inertial range. A Gaussian (dashed curve) is shown as a reference. (b) Hyperflatness factors as a function of scale, in the numerical experiment (DNS.I). Straight dashed lines represent Gaussian values. $s=\delta v/\langle \delta v^2\rangle^{1/2}$.

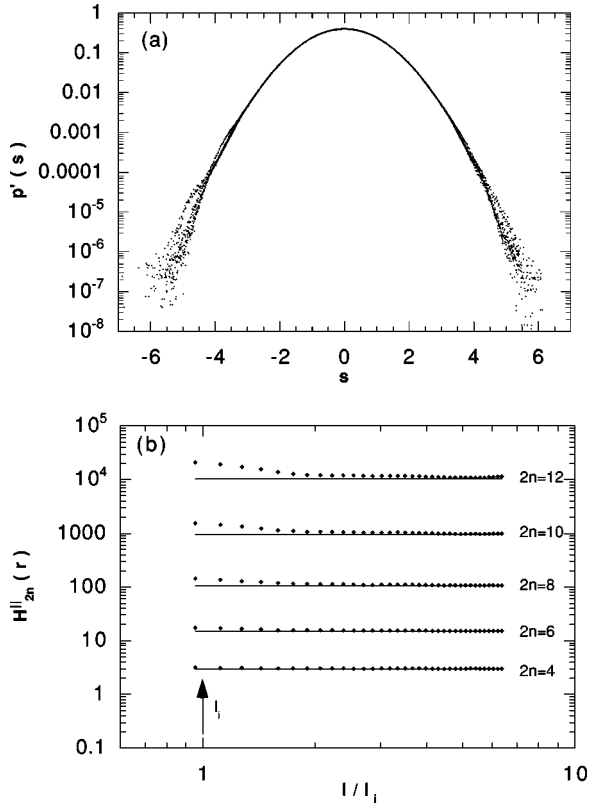

FIG. 4. Rescaled PDFs of longitudinal velocity increments for seven different separations in the inertial range (a), and hyperflatness factors as a function of scale (b), in the laboratory experiment (LE.I). Straight lines represent Gaussian values. $s=\delta v/\langle \delta v^2\rangle^{1/2}$.

nected to an energy transfer to scales larger than l and vice versa. For each position $\vec{x}$, one can define a circular control contour with center $\vec{x}$ and diameter l, and therefore a local flux $\varphi_l(\vec{x})$. As for the velocity increments, φ_l depends on time and position, and one can compute its moments and PDF. It follows from its definition and the incompressibility constraint that φ_l has a zero spatial average, so that we directly get the fluctuations of the energy flux. The intermittency signature will now be an eventual l dependence of the shape of its PDF.

We will always be interested in the l dependence of the shape of the PDFs. We therefore present normalized PDFs with variance one. Both the variable and its probability distribution are then dimensionless. The pressure could not be accurately measured in the experimental setup, hence we are unable to present transfer statistics for the laboratory experiments.

III. RESULTS

A. The inverse cascade regime, or small-scale structured turbulence

In the inverse cascade, there are long-lived structures, whose sizes are on the injection scale of the energy. The characteristics of such ''coherent'' structures have been analyzed in Ref. [3]. These vortices may merge from time to time (as shown in Babiano's simulation), but, at variance with the free-decay case, the merging process remains localized around the energy injection scale (if it was not so, enstrophy would be transferred at large scales, which is considered as unlikely in the inverse cascade). Owing to the presence of small-scale coherent structures, we may also call the inverse cascade regime ''small-scale structured turbulence.''

We focus here on the numerical and laboratory experiments (DNS.I) and (LE.I), where a statistically steady inverse energy cascade is achieved. Figures 3(a) and 4(a) show the PDFs of the two-point longitudinal velocity increments at separation length scales $l/l_I=2,5,10$ ($l_I=\pi/k_I$), encompassing the energy inertial range. The PDF are close to Gaussian at all scales in both cases. Numerical and experimental findings therefore agree and show that the intermittency correction remains small in the 2D inverse energy cascade. We emphasize on the fact that the prominent structures observed

in these stationary flows have a characteristic size of the order of the injection scale (see Figs. 1 and [9], respectively). We can characterize their importance by the ratio $R_v = l_v/L$ (l_v being the typical vortex size and L the box size) and their intensity $I_{v=}\omega_v/\omega_{rms}$ (ω_v being the typical vorticity at the core of vortices and ω_{rms} the root mean square of vorticity over the entire flow). We have $R_v \simeq 0.002$, $I_v \simeq 3$ for (DNS.I), and $R_v = 0.05$, $I_v \simeq 1.5$ for (LE.I).

Hyperflatness factors, defined by Eq. (3), are also represented in Figs. 3(b) and 4(b) for several orders of n up to $2n=12$ (thus corresponding to the 12th order moment of the distribution of the velocity increments). The dashed lines represent the Gaussian expectation at each order. One sees that up to $2n=6$ the numerical and experimental values are close to the Gaussian expectation throughout the inertial range. At higher order, there is a systematic deviation, which increases with the order, reaching 25% for $2n=12$, but they may be considered as within the error bar.

B. Condensation regime, or large-scale structured turbulence

In the condensation regime, there are long lived structures, whose sizes are on the box scale, or on the lattice mesh scale (for periodic boundary conditions). These vortices contain a substantial part, the energy of the system, since they are associated to a prominent peak in the energy spectra. Owing to the presence of such structures, we may also call the condensation regime as ''large-scale structured turbulence.''

The presence of large-scale structures in the condensation regime is visible in the numerical and laboratory experiments (DNS.III) and (LE.II); the long-lived vortices have a characteristic size *larger* than the injection scale [we now have $R_v \simeq 0.3$ for both experiments, $I_v \simeq 15$ for (DNS.III) and $I_v \simeq 7$ for (LE.II)]. Figure 5 shows PDFs of velocity increments for the two experiments and for three separations l ($l/l_I = 3,5,10$). In the case (DNS. III), the probability distribution functions strongly deviate from a Gaussian. This may be related with the large intensity of the strongest vortices (see Fig. 2). At the core of the vortices we have $\omega_v \simeq 15\omega_{rms}$. However, the observed deviation does not significantly depend on the separation length scale that may be contrasted with the fact that the dynamics (at least on large scales) is dominated by coherent structures. Figure 6 represents the corresponding hyperflatness factors. It can be seen that they are constant or slowly variable in the inertial range, corresponding again to the weakly scale-dependent shape of the PDFs.

We have an intermediate case displayed in the simulation (DNS.II), in which we have $R_v = 0.01$, $I_v \simeq 15$; the vortices are intense since the vorticity at their center is much larger (15 times) than the root-mean-square fluctuation of ω, as illustrated in Fig. 2. In this case, we observe far-from-Gaussian PDFs [Fig. 5(a)] that may be attributed to the presence of larger and more intense vortices. For comparison, in (LE.II) the PDFs are much closer to a Gaussian. The difference between the PDFs could be attributed to the different vortex properties: indeed, we only have in this case $\omega_v \simeq 7\omega_{rms}$ as one can see on the vorticity profile found in [9]

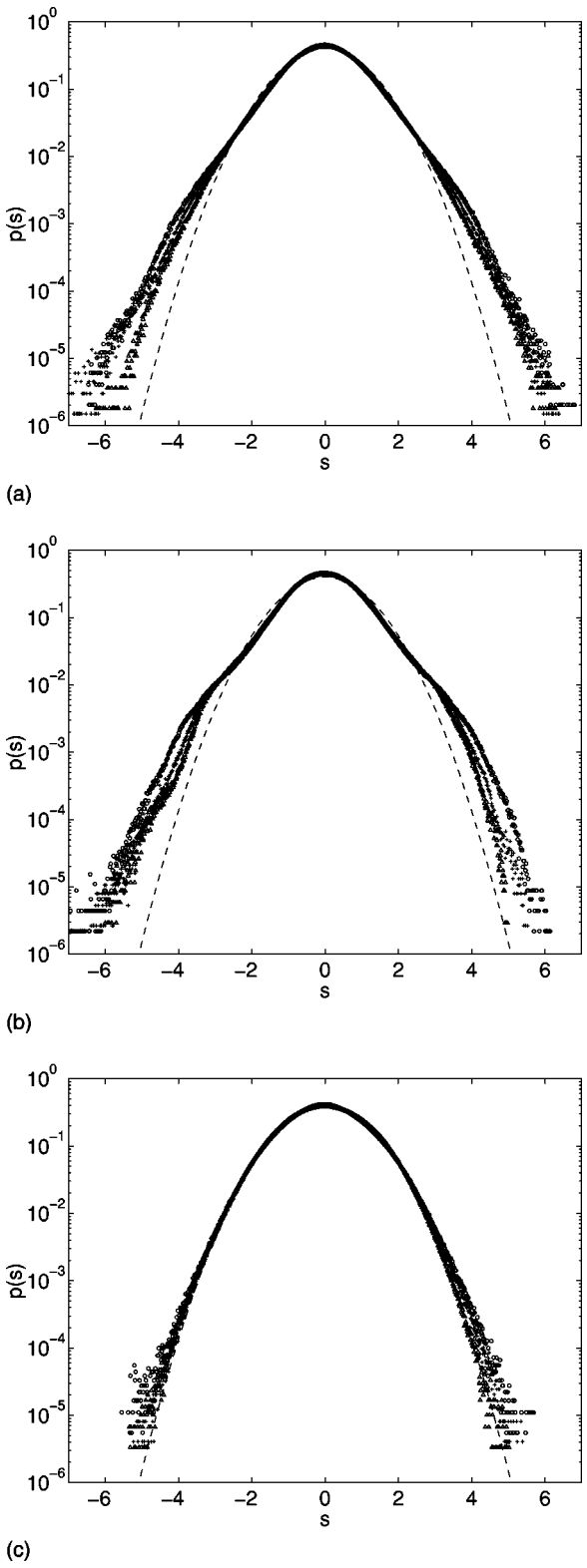

FIG. 5. Rescaled PDFs of longitudinal velocity increments for three different separations ($\ell/\ell_I = 3,5,10$) in the inertial range. A Gaussian (dashed curve) is shown as a reference. Experiments (DNS.II) (a), (DNS.III) (b), and (LE.II) (c). $s = \delta v/\langle \delta v^2 \rangle^{1/2}$.

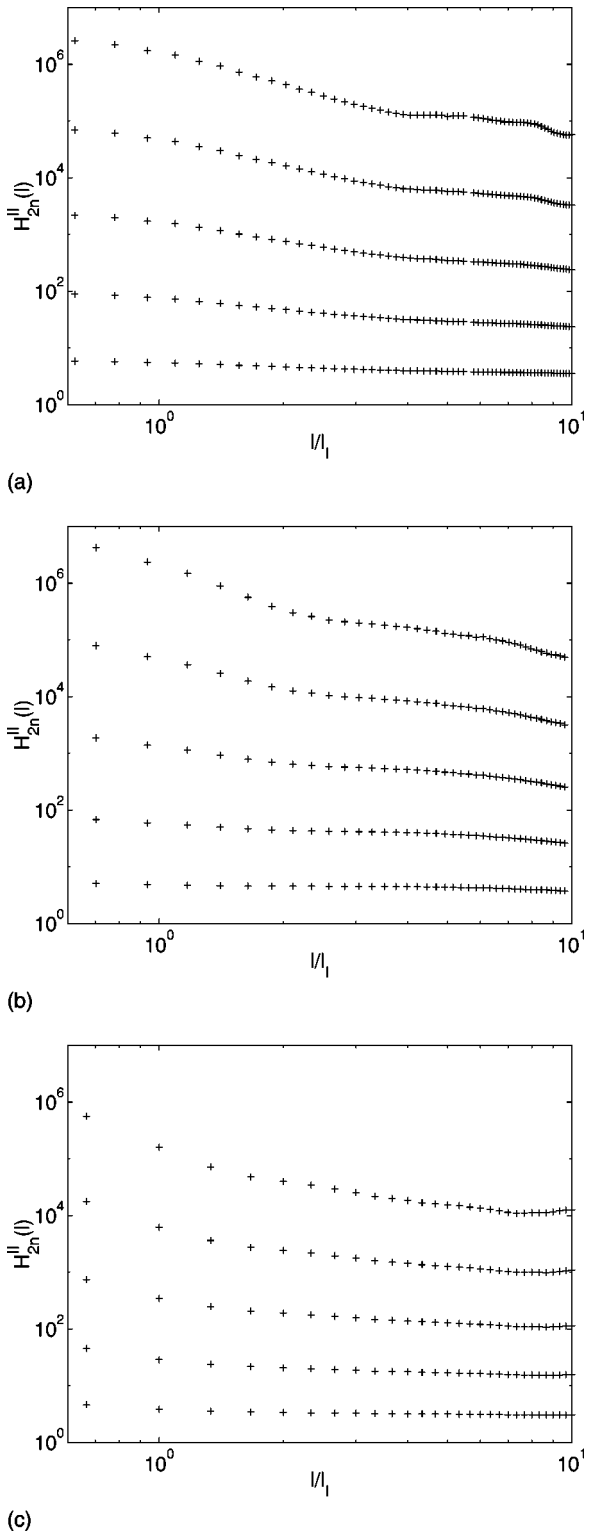

FIG. 6. Hyperflatness factors H_{2n} for $2n=4,6,8,10,12$ (from bottom to top) as a function of scale. Experiments (DNS.II) (a), (DNS.III) (b), and (LE.II) (c).

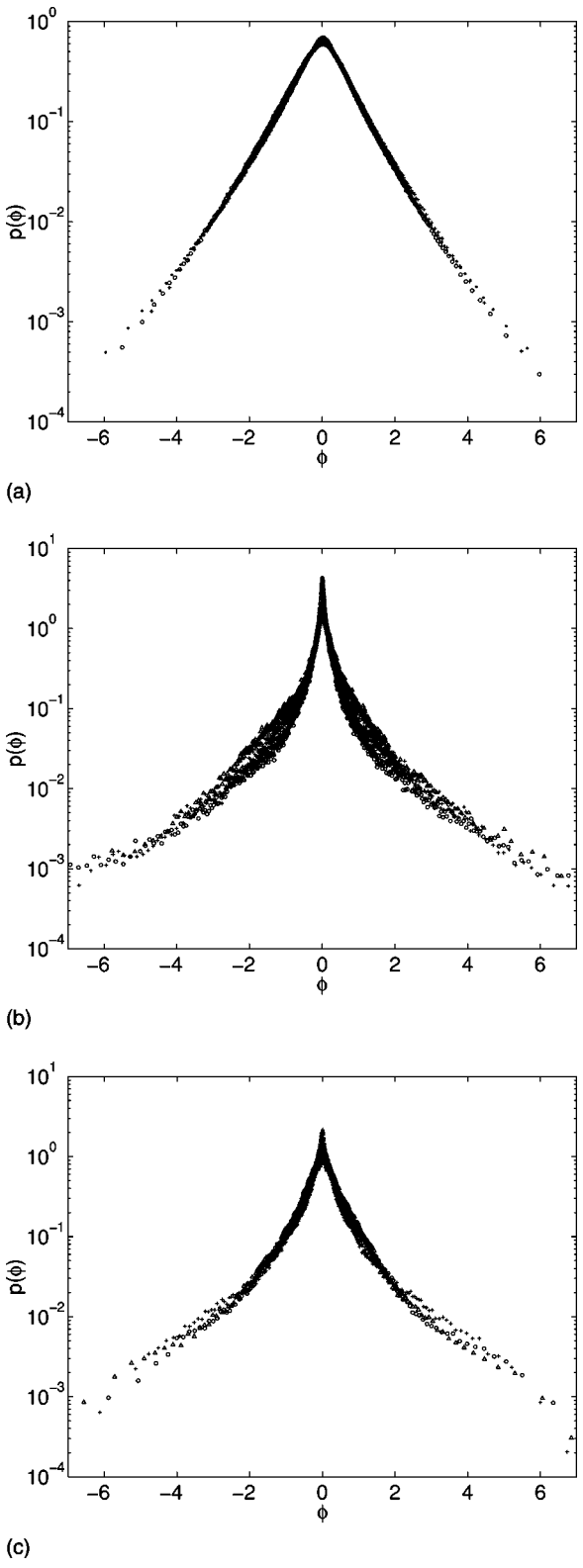

FIG. 7. Rescaled PDFs of energy transfer for three different separations ($\ell/\ell_I=3,5,10$) in the inertial range. Experiments (DNS.I) (a), (DNS.II) (b), and (DNS.III) (c). $\phi=\varphi_l/\langle\varphi_l^2\rangle^{1/2}$.

These structures coexist with a inverse cascade regime, characterized by a classical spectrum and a constant transfer of energy across the scales. The hyperflatness factors still weakly depend on l throughout the entire range of scale we consider, as can be seen in Fig. 6(a).

C. Transfer statistics

We consider here numerical experiments. We computed the energy flux φ_l in experiments (DNS.I), (DNS.II), and (DNS.III), at scales similar to those presented above. For simplicity, we actually integrated over square control contours. The resulting PDFs are presented in Fig. 7. All three PDFs are roughly symmetric, showing that the net inverse cascade flux results from the compensation of much larger inverse (positive) and direct (negative) fluxes. We stress the fact that one does not expect in any case these PDFs to be Gaussian. Indeed, φ_l is related through Eq. (4) to the pressure and to the third power of velocity increments, so that even if the latter are Gaussian, φ_l will not, due to this nonlinearity. This is the case for (DNS.I).

The shape of the PDF is not the same in the three experiments. This could be expected, since the statistics of the velocity increments strongly differ. In addition, the pressure may have a different contribution in the three experiments. Despite these differences one can see in all three cases a very weak l dependence of the shape of the PDFs. This is best verified in experiments (DNS.I) and (DNS.III). For (DNS.II), although its center and tails do not depend on the scale, one can observe a scale dependence of the PDF in the region where the value of φ_l is close to its root mean square. This point would deserve special attention, but is out of the scope of the present article. This dependance is anyway much smaller than the scale dependance of the PDF of the velocity increments in an intermittent cascade, like the 3D direct energy cascade. Therefore the observed weak scale dependence of these PDFs essentially confirms the conclusions drawn from the statistics of the velocity increments.

IV. CONCLUSION

The numerical and experimental results presented in this work are consistent; the two approaches confirm that there is no sizeable internal intermittency in the two-dimensional inverse energy cascade. This situation contrasts with the three-dimensional case. In the experiments we analyzed, the absence of intermittency is observed even in the condensation regime, where coherent vortices dominate the large scales of the system. The PDF of the velocity increments are non-Gaussian, and the hyperflatness remains constant in the inertial range. Considering directly the energy transfer statistics confirms these results. The deviations from Gaussianity are probably associated to the presence of large-scale coherent structures. Nevertheless, and this is our main point, these deviations from Gaussianity are not associated with any measurable internal intermittency.

ACKNOWLEDGMENTS

We thank M. Vergassola and G. Falkovich for discussions concerning this work and M. C. Jullien for her help concerning the experimental data. This work was supported by École Normale Supérieure, Universités Paris 6 and Paris 7, Centre National de la Recherche Scientifique, and by EEC Network Contract No. FMRX-CT98-0175.

[1] M. Rutgers, Phys. Rev. Lett. **81**, 2244 (1998).
[2] J. Sommeria, J. Fluid Mech. **170**, 139 (1986).
[3] J. Paret and P. Tabeling, Phys. Rev. Lett. **79**, 4162 (1997).
[4] R. Kraichnan, Phys. Fluids **10**, 1417 (1967)
[5] U. Frisch and P. Sulem, Phys. Fluids **27**, 1921 (1984).
[6] J. Herring and J. McWilliams, J. Fluid Mech. **13**, 229 (1985).
[7] A. Babiano, B. Dubrulle, and P. Frick, Phys. Rev. E **52**, 3719 (1995).
[8] G. Boffetta, A. Celani, and M. Vergassola, Phys. Rev. E **61**, 29 (2000).
[9] J. Paret and P. Tabeling, Phys. Fluids **10**, 3126 (1998).
[10] L. Smith and V. Yakhot, J. Fluid Mech. **274**, 115 (1994).
[11] V. Borue, Phys. Rev. Lett. **72**, 1475 (1994).
[12] C. Basdevant, B. Legras, R. Sadourny, and M. Beland, J. Atmos. Sci. **38**, 2305 (1981).
[13] J. Paret (unpublished).
[14] A. Babiano, B. Dubrulle, and P. Frick, Phys. Rev. E **55**, 2693 (1997).